

# Simple Networks for Spike-Timing-Based Computation, with Application to Olfactory Processing

Carlos D. Brody<sup>1,3,\*</sup> and J.J. Hopfield<sup>2,3,\*</sup>

<sup>1</sup>Cold Spring Harbor Laboratory  
P.O. Box 100  
Cold Spring Harbor, New York 11724  
<sup>2</sup>Department of Molecular Biology  
Princeton University  
Princeton, New Jersey 08544

## Summary

Spike synchronization across neurons can be selective for the situation where neurons are driven at similar firing rates, a “many are equal” computation. This can be achieved in the absence of synaptic interactions between neurons, through phase locking to a common underlying oscillatory potential. Based on this principle, we instantiate an algorithm for robust odor recognition into a model network of spiking neurons whose main features are taken from known properties of biological olfactory systems. Here, recognition of odors is signaled by spike synchronization of specific subsets of “mitral cells.” This synchronization is highly odor selective and invariant to a wide range of odor concentrations. It is also robust to the presence of strong distractor odors, thus allowing odor segmentation within complex olfactory scenes. Information about odors is encoded in both the identity of glomeruli activated above threshold (1 bit of information per glomerulus) and in the analog degree of activation of the glomeruli (approximately 3 bits per glomerulus).

## Introduction

Consider a rat inhabitant of the New York City subway, scurrying along the tracks in search of food. For olfaction to be a useful modality in this endeavor, the rat must be able to recognize distant odors. But food odors in the natural world will rarely exist alone—they will usually be experienced in the context of a large variety of other odors also present in the environment. Thus, the rat must be able to *segment*, or separate, a known odor from its olfactory background (similar to the way an experienced cook may identify, by smell, a particular spice used in a soup). Furthermore, the rat will experience an odor at various distances from the source, implying that it is sensed at many different concentrations. Yet all these different concentrations must be interpreted as coming from the same odor source; odor recognition must thus be significantly *concentration invariant*. Experiments show that humans can recognize 3–4 individual components of a mixture (Laing and Francis, 1989; Laing and Jinks, 2001) and have concentration-invariant recognition of odors over a range as large as

a factor of 100 in concentration (Krone et al., 2001). Highly olfactory animals such as rats are likely to have greater capabilities.

Hopfield (1999) proposed an abstract algorithm that simultaneously addressed these three problems (recognition, segmentation, concentration-invariance). Here we describe how this abstract algorithm can be instantiated in a network of spiking neurons, using an architecture similar to that of the mammalian olfactory bulb. The key neural computation used was introduced previously (Hopfield and Brody, 2000, 2001) and might be termed many-are-equal (MAE). In MAE, a large set of neurons synchronize their spiking when the inputs to the neurons are approximately equal. We show how the problem of concentration-invariant odor recognition can be transformed into a problem that can be solved using MAE. When an odor is present, different olfactory receptor neuron classes are activated to different degrees. For each odor that is to be recognized as a known odor, the essential step is to transform the different relative activations into a uniform pattern, which can then be recognized by MAE. Our simulations show that a spiking neural network built on these principles can achieve a high level of odor discrimination over a 50-fold range in concentration and can do so in the presence of a distracting background odor stronger than the target.

MAE itself may be instantiated through a variety of mechanisms. In the present paper, the synchrony comes about due to an underlying common oscillatory drive. By contrast, in a previous system (Hopfield and Brody, 2000, 2001), the synchronization underlying MAE resulted from direct synaptic interactions between neurons. While these two mechanisms are mathematically related, the common oscillatory drive mechanism is both more relevant to olfactory systems and easier to understand and control from a theoretical perspective.

Our approach is not to develop highly detailed models that mimic all features of a biological olfactory system. Rather, we have tried to develop a model that most clearly and simply illustrates the essence of the computations. Many features of the model have been directly inspired by properties of biological olfactory systems. In particular, the basic architecture (e.g., input dimensionality, convergence/divergence) has been chosen to match that of the mammalian olfactory bulb. As shorthand for communication, we therefore sometimes use biological terms to refer to matching concepts in the model (e.g., “glomeruli” encode the activity of a single receptor type, and each glomerulus provides the principal input to a number of “mitral cells”). When successful, such simplified models can be used as guides for later development of more detailed and biological models. For example, the common subthreshold oscillatory drive, observed in the primary stages of biological olfactory systems and used here, could be created in a variety of ways: through an external oscillator, through an embedded oscillating network, or through feedback synaptic connections between the synchronizing neurons themselves. However, elucidation of the specific mecha-

\*Correspondence: brody@cshl.org (C.D.B.), hopfield@princeton.edu (J.J.H.)

<sup>3</sup>These authors contributed equally to this work.

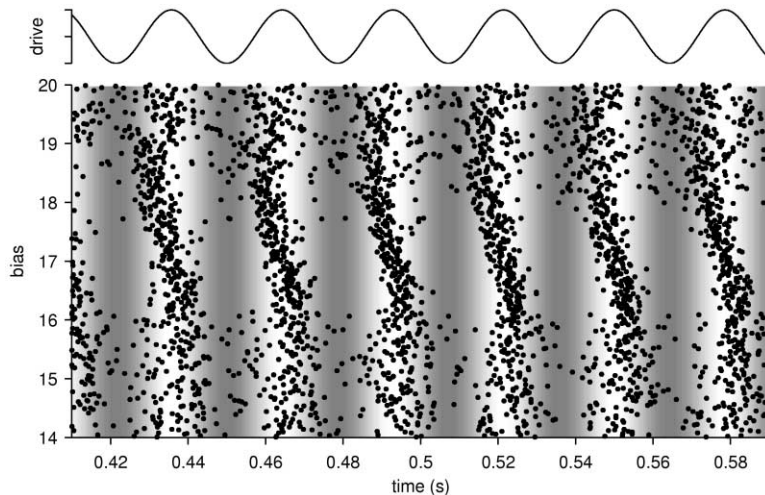


Figure 1. Action Potential Rasters for Integrate-and-Fire Neurons in the Presence of a Subthreshold Sinusoidal Current Injection

Each row represents a neuron, and each neuron has a different DC current injected into it, indicated by the ordinate. Dots indicate the time of action potentials. The common sinusoidal input current is indicated in the upper plot and by the grayscale shading underlying the action potential rasters. Gaussian noise is injected into each cell. There is a range of DC currents that result in approximate phase-locking, with phase progressing in an orderly and almost linear fashion along this current range. The cell time constant was 20 msec, and the drive frequency 35 Hz.

nism responsible for such an oscillation is not necessary at this computational level of analysis.

We will first describe the properties of the synchronization mechanism used here, and then turn to the use of MAE in the problem of olfaction.

## Results

### The Basic Synchronization Phenomenon

A nonadapting neuron that is driven by an oscillating subthreshold potential plus a constant current input can phase lock its action potentials with the oscillating potential. This phenomenon is responsible for the phase locking of the action potentials coming from the cochlear nucleus neurons in response to low-frequency tones (Lavine, 1971; Johnson, 1980). It is a phenomenon of most neural models, including Hodgkin-Huxley neurons (simulation not shown) and integrate-and-fire neurons. There is a range of strengths of the constant current input at which the phase locking will be 1-to-1 in the sense that each cycle of the oscillation will contain one spike from the neuron. In the absence of noise, the phase of this spike with respect to the underlying oscillation will be precisely determined by the strength of the constant current input.

In the presence of noise, the phasing will no longer be precise, but there will nevertheless be a tendency to fire at a specific phase. Figure 1 shows the phase locking of integrate-and-fire neurons having different current inputs in the presence of a common sinusoidal input current. The level of noise used here and throughout the simulations in this paper was chosen to roughly match the precision of phase locking observed in rat olfactory bulb slices (Desmaisons et al., 1999) and rabbit olfactory bulb in vivo (Kashiwadani et al., 1999). Matlab code to generate this and other figures is available at <http://www.cshl.edu/labs/brody/nose>.

These phase-locking properties can be used to construct an MAE operation. If many neurons are all receiving a current input that is within the 1-to-1 phase-locking range, and all of these input currents are similar, then the neurons will all be firing at a similar phase with

respect to the underlying oscillation. The neurons will therefore all be synchronized to each other. In contrast, if the neurons receive constant current inputs that are different from each other, or that are not within the 1-to-1 phase-locking range, then the spike timing synchronization across neurons will be much weaker. Thus, as in our previous network (Hopfield and Brody, 2000, 2001), similarity of inputs is signaled by synchronization of action potentials. In the present network, however, synchronization across neurons is achieved through synchronization to a common underlying signal, instead of being achieved through direct neuron-to-neuron synaptic interactions.

A comparison of the MAE operation, computed through two different synchronization-promoting mechanisms, is illustrated in Figure 2. The left half of this figure illustrates phase locking via "horizontal" connections as presented in earlier work; the right shows the same MAE operation computed by a network without horizontal connections, but using instead a common input subthreshold current to produce synchronization. Similar synchronization is seen with both mechanisms, although there are differences. For example, the interspike separation when well synchronized is always the reciprocal of the period of the common drive in one case (right column), while it depends on the current level at which the currents converge in the other (left column).

### Odor Recognition

The essential idea behind the algorithm proposed by Hopfield (1999) is based on the fact that there is a large family of odor receptors cell types, numbering approximately 1000. Each receptor cell class responds to many different odors (Sicard and Holley, 1984; Buck, 1996), and any particular odor thus activates, in a concentration-dependent manner, a substantial subset of these receptors (on the order of hundreds of receptor cell types). In the rat, each glomerulus in the olfactory bulb receives input from  $\sim 10,000$  sensory cells (Shepherd and Greer, 1998), each of which expresses a single type of receptor protein (Buck and Axel, 1991). There are  $\sim 1000$  glomerular types, corresponding to the number

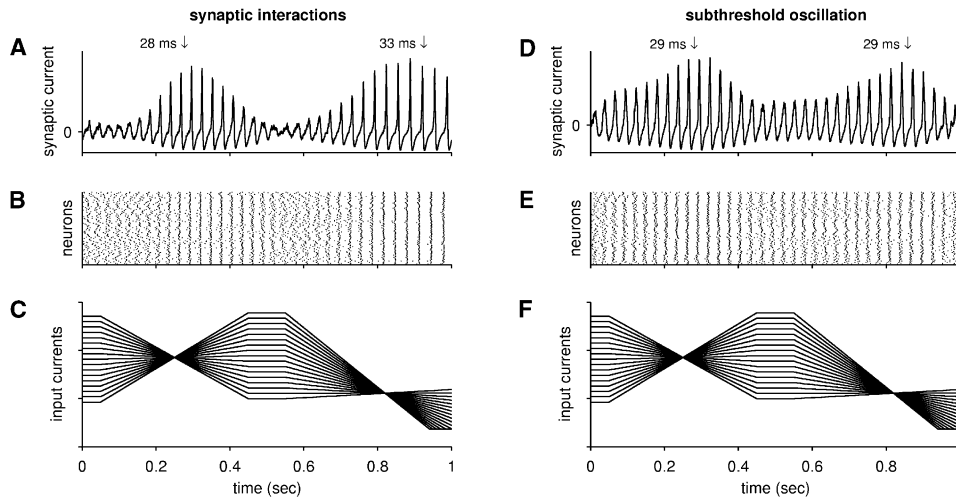


Figure 2. Two Different Synchronization Mechanisms Lead to Similar Results

Many-are-equal synchrony, indicating that the input currents to many cells are about the same, implemented through two different mechanisms: “horizontal” synaptic interactions between a set of cells (A–C), versus a common input sinusoid to otherwise independent cells (D–F). Each cell in (B) and (E) has a time-dependent current injected into it; the currents for these cells are shown in (C) and (F). The spike rasters and their movement into and out of synchronization are shown in (B) and (E). The synchrony is also illustrated in (A) and (D), which show the membrane potential of a neuron that receives both excitatory (synaptic currents exponential,  $\tau = 2$  ms) and inhibitory ( $\alpha$  function currents,  $\tau = 6$  ms) input currents from the spike rasters shown in (B) and (E), respectively. For (A) and (D), the cell time constant is 6 ms. In (D)–(E), the underlying input frequency is 35 Hz. In (B) and (E), the ordering of the spike rasters has been randomly chosen.

of receptor cell types. The primary dendritic branches of a single mitral cell in the olfactory bulb lie largely within one glomerulus, and many different mitral cells share a single glomerulus (Shepherd and Greer, 1998).

Here we will call the different mitral cells of a glomerulus the “glomerular repertoire” corresponding to a receptor type (Figures 3 and 4A). We propose that during

odor recognition, the many neurons within a glomerular repertoire are all similarly driven by activation of their receptor cells, but in addition have different positive bias currents driving them (Figures 3 and 4B). Here, a diversity of bias currents was obtained by assigning a random bias current to each repertoire cell, the magnitude of which was then assumed to be a fixed property

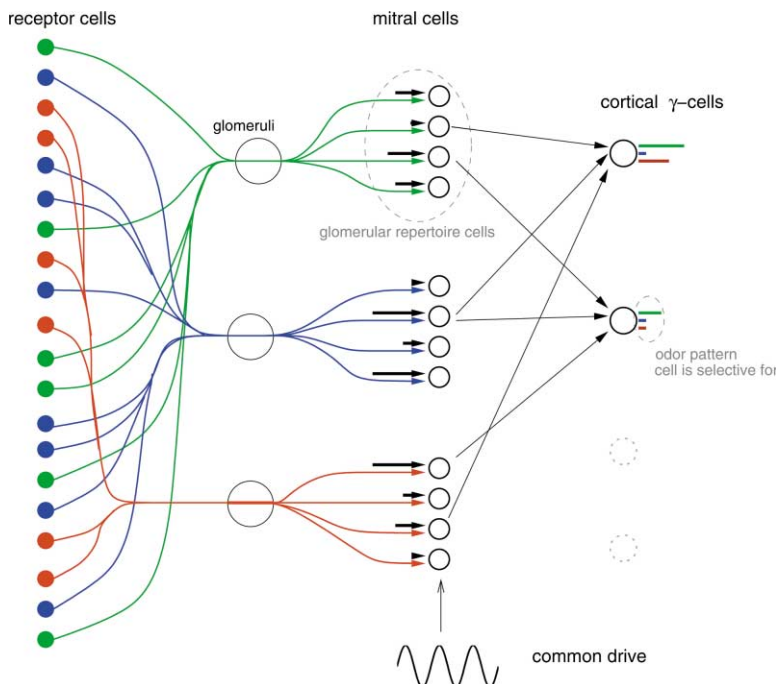


Figure 3. The Structure of the Model Olfactory System

The left layer of cells represent three different classes of receptor cells, with outputs converging in each case to a single glomerulus. The middle layer of cells represents the mitral cells of the olfactory bulb. The thick black arrows represent bias currents (to be described below). The right layer of cells represents cells of pyriform cortex, and the colored bars represent the pattern of olfactory stimulation which will be recognized, lock-and-key fashion, by a cortical cell that receives synaptic input from the mitral cells indicated by the long thin arrows. In the simulations, 400 different receptor classes were used, and each glomerulus had 14 mitral cells.

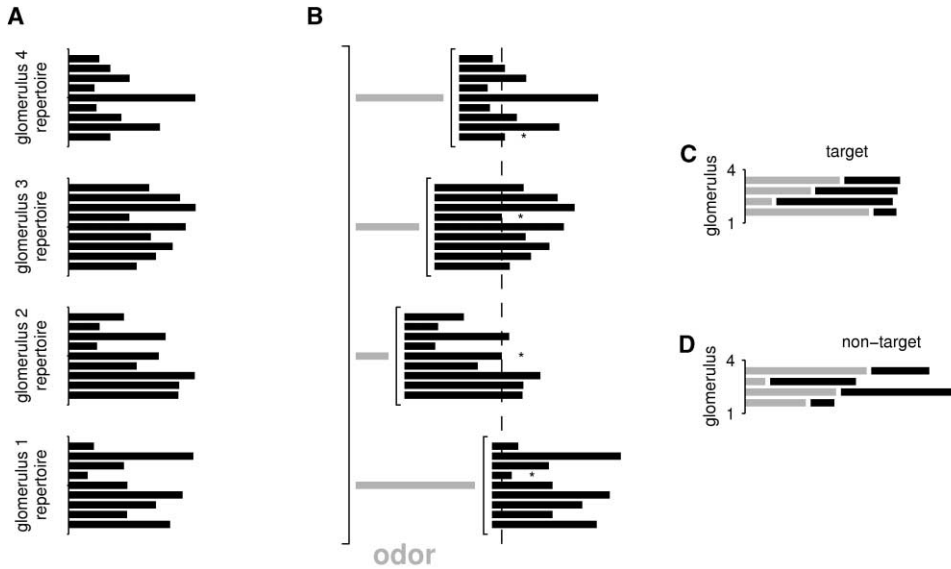


Figure 4. Glomerular Repertoire and Many-Are-Equal Odor Recognition

(A) Each glomerulus has a set of repertoire cells, each of which is driven by a fixed but random bias current, with strength represented by the length of a black bar.  
 (B) An odor that activates the four illustrated glomeruli above threshold. The length of the gray bars indicates the degree of activation drive for each glomerulus. The *total* input current to each of the repertoire cells is its bias current plus its sensory current, and is represented by the location of the right ends of the black bars. We can find a set of repertoire cells, designated by asterisks, that all have total input current near to the same value (vertical dashed line); these can be used for recognition of this particular odor through the MAE operation.  
 (C) Sum of receptor activation plus selected repertoire cell bias currents (asterisked bars in B) for a target odor.  
 (D) Sum of receptor activation plus selected bias currents for a nontarget odor.

of the cell. Many insects, including the locust, lack the large repertoire of output neurons per glomerulus characteristic of vertebrates; the algorithms and neural implementations that characterize these systems may differ from those of the rat.

Now, consider a particular odor that generates an analog pattern of glomerular activation. If each glomerulus has a repertoire of “mitral” cells driven by random bias currents as in Figure 4A, we can find a set of repertoire cells (asterisks in Figure 4B) that receives, in addition to the receptor drive, a bias current such that the sum of the receptor and bias currents is similar, across glomeruli. Presentation of the target odor will then lead to similar net activation across the selected cells (Figure 4C), while a different, nontarget odor would lead to quite diverse activations across the selected cells (Figure 4D). In essence, the set of bias currents of the selected mitral cells acts as a “lock” that corresponds to the “key” of receptor activations for a specific (target) odor. The problem of odor recognition has thus been transformed into an MAE problem: the target odor is deemed present when many of the selected mitral cells have net activations (receptor + bias) that are closely similar to each other.

One of the key problems to be addressed is concentration-invariant odor recognition. We must therefore define how receptor coverage and glomerular drive depends on concentration. Let  $i$  refer to index receptor types, and let the coverage  $r_i$  of receptor type  $i$ , in the presence of odor  $o$ , be given by

$$r_i = c_o k_{oi},$$

where  $c_o$  indicates the concentration of odor  $o$  and  $k_{oi}$  is a constant that depends on both receptor type and odor identity. The response defines a  $\sim 1000$ -dimension odor vector having components  $r_i$ . The net signal reaching the mitral cells in the glomerulus corresponding to receptor type  $i$  will be denoted  $s_i$ . Following Hopfield (1999), we assume that  $s_i$  encodes odor concentration in a roughly logarithmic fashion, that is:

$$s_i = k \log(1 + c_o k_{oi}/\theta). \quad (1)$$

This is approximated by a threshold-logarithmic function

$$s_i \approx 0 \text{ for } c_o < \theta/k_{oi} \\ s_i \approx k \log(k_{oi}/\theta) + k \log(c_o) \text{ for } c_o > \theta/k_{oi}, \quad (2)$$

where  $k$  is the same for all receptor types, and  $\theta$  is the receptor coverage necessary for a just-detectable glomerular signal. Both electrophysiological studies of olfactory receptor neurons (Duchamp-Viret et al., 2000) and optical imaging of glomeruli (Rubin and Katz, 1999; Meister and Bonhoeffer, 2001; Wachowiak and Cohen, 2001) suggest that, over a range of roughly 100- to 1000-fold change in concentration, glomerular activation is a logarithmic function of odorant concentration. At very low concentrations ( $c_o < \theta/k_{oi}$ ), the receptors fail to respond. For very large concentrations, the receptors appear to saturate. Here, concentrations were generally kept in the region corresponding to the lack of firing below a threshold and the logarithmic range above threshold. Saturation at the top of the range was omitted for simplicity.

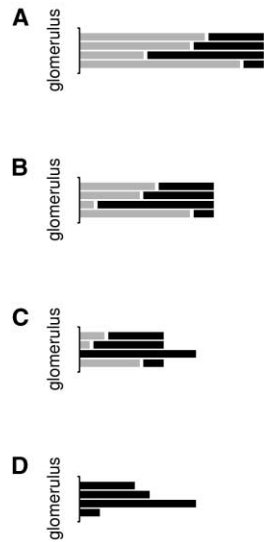


Figure 5. Activation of Selected Mitral Cells for a Target Odor when that Odor Is Presented at Different Concentrations

Same conventions as in Figure 3A. (A)–(D) illustrate presentation of the target odor at successively lower concentrations. At the very lowest concentration (D), none of the illustrated glomeruli are driven above threshold, and the mitral cell activities reflect only their bias currents.

Below we will loosely refer to  $s_i$  as the glomerular activation corresponding to receptor type  $i$ . Logarithmic encoding above threshold implies that a change in the concentration of an odor will lead to an additive change in  $s_i$  across all above-threshold glomeruli. Figures 5A–5D show the receptor + bias activations for a set of mitral cells driven by their target odor at different concentrations. At the highest concentrations (Figures 5A and 5B), a change in concentration leads only to a change in the common level at which the mitral cells are driven: similarity of net drive across mitral cells is preserved on concentration changes. Thus, odor recognition based on the MAE operation will be concentration invariant. As concentration falls further, some receptors fall below threshold (Figure 5C); corresponding mitral cells cease having a net drive similar to the others in the selected set. Since the MAE operation is robust to outliers, correct odor recognition will still be possible. At very low concentrations, where most receptors are below threshold, most mitral cells are driven only by their bias currents, and recognition is no longer possible (Figure 5D).

So far, we have described *concentration-invariant odor recognition*. *Odor segmentation* can be achieved by noticing that odors typically activate strongly only a subset of the available receptor types. Even if a strong distractor odor drives most of the target odor’s receptor types above threshold, when both the distractor and the target are present, the relative activations of a significant fraction of the target’s receptor types will be dominated by the target odor, allowing recognition of the target odor separately from the background. We explore this point more fully in the simulations of Figure 6B below.

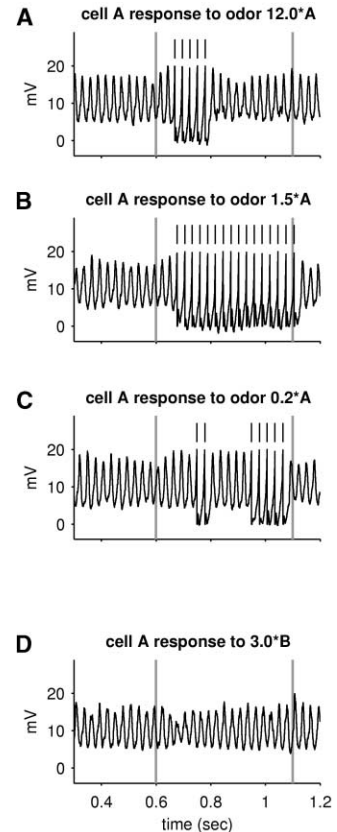


Figure 6. Odor-Selective, Concentration-Invariant Responses of a  $\gamma$  Cell

(A–C) Response of a  $\gamma$  cell designed to be selective for odor A, upon presentation of odor A at three different concentrations. The solid line represents the membrane potential of the  $\gamma$  cell. Spiking threshold is 20 mV; small vertical lines above the membrane potential indicate spikes. Vertical gray lines indicate the beginning and end of the 0.5-s-long odor presentation.

(D) Response of same  $\gamma$  cell upon presentation of a different, random, odor B.

### Simulation of a Network of Neurons for the Model Olfactory Problem

The tasks described above can be successfully performed by a network of spiking neurons. Since we are unable to examine the spiking system analytically, we instead performed extensive simulations using simple integrate-and-fire units. Our goal is to provide a proof-of-concept that noisy spiking neurons, using the MAE operation, can (1) achieve highly odor-selective synchronization; (2) do so in a manner invariant to a wide range of odor concentrations; and (3) do so in the presence of strong background distracting odors. In addition, we used the results of the simulations as the basis for evaluating what information about the odor vector is used in the network decision.

In our simulated network, there were “odor inputs” from 400 glomeruli. Each glomerulus had its own ensemble of repertoire cells, with a range of steady bias currents. The bias currents for repertoire cells (Figure 4A) were chosen at random from the range of bias currents

shown in Figure 1. For most of the simulations, 14 repertoire cells were assigned to each glomerulus.

All repertoire cells, in all glomeruli, were also driven by a common oscillatory input current at 35 Hz. The total input to a repertoire cell  $n$  in glomerulus  $i$  was thus

$$I_i^{\text{sensory}} + I_{n,i}^{\text{bias}} + I^{\text{periodic}} \cos(\omega t),$$

where  $I_i^{\text{sensory}}$  for each glomerulus was linearly proportional to  $s_i$  of Equation 2. The repertoire cells were modeled as single compartment integrate-and-fire neurons with 20 ms time constants. Gaussian random noise was injected into each cell.

The odor stimulus, represented by the set of activations  $s_i$ , was a single “sniff” lasting 0.5 s. Mammals often sniff more rapidly than this, but may use multiple sniffs in making decisions. Half of a second was chosen in order to simulate a sniffing phenomenon, while getting enough information in a single sniff to make multiple sniffs unnecessary. For a single odor, the set of receptor coverages for an odor  $A$ ,  $r_i = c_A k_{A,i}$ , was modulated by an overall “sniff.” When two odors, A and B, are present in a single sniff, their receptor coverages add (see Experimental Procedures).

Synchrony across chosen subsets of repertoire cells (e.g., starred repertoire cells in Figure 4C) is the event that indicates recognition of a specific odor. To indicate synchrony, we used “reporter”  $\gamma$  cells, which were also modeled as single-compartment integrate-and-fire units (see Experimental Procedures), and which received synaptic input from the chosen subset of repertoire cells (Figure 3).

It is unlikely that biology uses single-cell responses to correspond to single odors. We use a “grandmother cell” representation of an odor as a surrogate of a “highly selective cell” in neurobiology. In the  $\gamma$  cell representation, there is no limit to the number of odors that could be separately recognized, each by its own  $\gamma$  cell. In actuality, biology is much more likely to find a combinatorial representation of odors, although it should be noted that very highly odor-selective cells have recently been reported in mushroom bodies of locust (Perez-Orive et al., 2002). Mushroom bodies have a location in the olfactory circuitry of an insect that is analogous to that of pyriform cortex in mammals.

The analog information about the relative strengths of the components of an odor are “stored” in the choice of which repertoire cells to use, not in the strength of the connections.

### Results of Simulations

We now show that a  $\gamma$  cell’s spiking is highly odor specific, responding only to its target odor over a wide range of concentrations and recognizing its odor in the presence of strong distractor scents. The relative activations of different glomeruli, rather than merely the binary pattern of active versus inactive glomeruli, are essential to perform the desired olfactory tasks.

Figure 6B illustrates the behavior of a  $\gamma$  cell designed to recognize an odor labeled A, in response to a presentation of A at concentration 1.5. The  $\gamma$  cell spikes robustly. In contrast, in response to a different odor, B, at a concentration of 3.0, the  $\gamma$  cell does not fire any spikes (Figure 6D). Figure 6A illustrates the response of

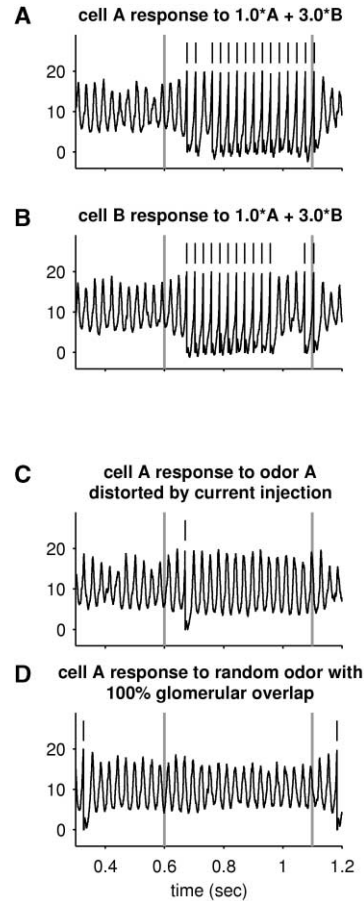


Figure 7. Odor Selectivity and Odor Segmentation

Same format as Figure 6.

(A) Response of a  $\gamma$  cell selective for odor A upon presentation of its target odor plus a stronger background odor.

(B) Response of a  $\gamma$  cell selective for the background odor B.

(C) Response of  $\gamma$  cell selective for odor A upon presentation of a distorted odor A (see text).

(D) Response of  $\gamma$  cell selective for odor A upon presentation of a random odor that has 100% overlap with odor A of glomeruli driven above threshold.

the  $\gamma$  cell to a much higher concentration of odor A; Figure 6C illustrates the response to a much lower concentration. Recognition events defined as four or more spikes from the A-selective  $\gamma$  cell are invariant to at least a 50-fold range of concentrations. We have not investigated the ultimate odor selectivity of the system here, but empirically we examined the response of an odor-selective  $\gamma$  cell to 3,000,000 nontarget random odors at concentration 1.5. For computational efficiency, we used smaller, and therefore less selective, systems (the selectivity increases rapidly with the number of glomeruli). At 280 glomeruli, none of the  $3 \times 10^6$  random odors examined generated even a single  $\gamma$  cell spike during the sniff in response. A 400 glomerulus system would be even more selective. Requiring four spikes for odor identification is thus an extremely conservative criterion, given the unresponsiveness of the A-selective cell to random odors.

Figure 7A shows the response of a  $\gamma$  cell selective to

odor A when presented with a mixture of odor A at concentration 1.0 and odor B at concentration 3.0. This cell, which does not respond to B alone, does respond briskly to the mixture. By contrast, a cell which is responsive to a third random odor C will not respond to A, to B, or to this mixture (not shown). Similarly, in Figure 7B the  $\gamma$  cell selective for B responds to this mixture. These patterns indicate that a cell can identify its own target odor even in the presence of a background that is stronger than the target odor, and that this response is indeed the result of the presence of its target, not a general response of all cells to a complex mixture.

The analog strength of the glomeruli driven above threshold is essential in these concentration-invariant and background-resistant recognitions. They are not merely the result of using the pattern of glomeruli driven above threshold (which varies strongly with background odors that may be present and with concentration; Meister and Bonhoeffer, 2001). To demonstrate this, we constructed an odor A' that drove above threshold precisely the same set of glomeruli driven above threshold by odor A, but with different, random analog activations. Figure 7D shows that the A-selective  $\gamma$  cell did not fire any spikes in response to this "scrambled" odor A'. The binary pattern of above-threshold glomeruli does not describe the selectivity of this system: the *analog* pattern of activations is crucial.

Unlike a response based only on the identities of glomeruli driven above threshold, *increasing* the strength of the drive to above-threshold glomeruli can *decrease* the response of a  $\gamma$  cell. Figure 7C shows the behavior of an odor A-specific  $\gamma$  cell in response to odor A plus the injection of a common excitatory current into half of odor A's glomeruli. This current was equivalent to increasing the "effective concentration" driving the injected glomeruli by a factor of 4. The result is that the  $\gamma$  cell virtually ceases to generate action potentials, even though half of odor A's glomerular inputs were increased. This counterintuitive result comes about not by activation of an inhibitory pathway, but from the failure of all cells to share in a common phase of synchronization.

The analog aspect facilitates the analysis of mixtures (or rejecting backgrounds), an important olfactory task. Figure 7 indicates that two random odors, A and B, that activate only partially overlapping sets of glomeruli can be individually recognized in the mixture 1·A + 3·B. We have also examined this separation problem in the much more difficult case, when odors A and B are chosen so that they drive exactly the same glomerular set. The decomposition is nonetheless successfully carried out by the network. The  $\gamma$  cell for odor A responds somewhat less robustly than in the completely random case, but typically produces ~5 spikes in response to 1·A + 3·B, yet produces zero spikes in response to B alone (data not shown). In this case, all three of A alone, B alone, and 1·A + 3·B have exactly the same pattern of glomeruli driven above threshold. Odor recognition based only on the pattern of glomeruli activated above threshold cannot accomplish this task, nor can it explain the capacity of the network to deal with this problem.

The higher the number of similarly activated mitral cells connected to a  $\gamma$  cell, the more strongly they will drive the  $\gamma$  cell. We can choose connection strengths and thresholds for the  $\gamma$  cell such that strong firing will

result if half or more of the mitral cells are synchronized. This allows high odor selectivity, since it is highly unlikely that a random odor would match a subset of this size. At the same time, this threshold level allows significant robustness, since any half of the receptor set may be corrupted without disrupting odor recognition (Hopfield, 1995; Hopfield et al., 1998).

### The Quantity of Analog Information Used

In the system we have described, information about odor identity is carried in both the pattern of activation (which describes only the identity of the set of glomeruli driven above a fixed threshold of activation) and the analog activation (the quantitative strengths of activation of the glomeruli that are driven above a threshold level). Many common olfactory tasks would appear to be difficult to perform using pattern information alone. For example, a rich background odor mixture that activated all glomeruli above threshold would preclude identifying the presence of any other odor (or any known components of the background itself) if the only information available were the identity of activated glomeruli. Similarly, two odors that drove the same set of glomeruli above threshold could not be distinguished. In contrast, our system makes use of the analog information, and this allows it to readily perform behaviorally significant tasks that would be impossible on the basis of pattern alone (e.g., Figure 7D). For this reason, it is significant to make a quantitative assessment of the amount of analog information our system makes use of. Note that we are not asking how many different odors the system can distinguish, but merely asking what precision is significant at the input to the system.

We approached this problem by asking with what precision a test odor must match the analog strengths of its target in order to produce an adequate recognition response from the  $\gamma$  cell. (If test and target activate the same glomeruli above threshold, how similar must test and target be?) This precision can be rephrased in terms of the number of bits with which each analog component must be specified.

We picked a random target odor and constructed a  $\gamma$  cell designed to recognize precisely that target. We then tested the response of the  $\gamma$  cell to odors that differed from the target, while activating the same glomeruli above threshold as the target. For example, the strength of each of the chosen components for the test odor could be set entirely at random, chosen from a uniform distribution over the full range of possible glomerular activation levels. This represents no knowledge of the analog strength of that component in the target odor, and the analog information present was then zero bits. Alternatively, each component of the test odor could be chosen in a biased random fashion so that it had some information about the size of the component of the target odor, but randomness to the extent that the test ensemble contained (on average)  $n$  bits of information about each component. As the number of bits goes up, the average squared difference between the typical test component and the matching target odor component drops, so that the square root of this average (rms distance) falls by a factor  $\sim 2^{-n}$ .

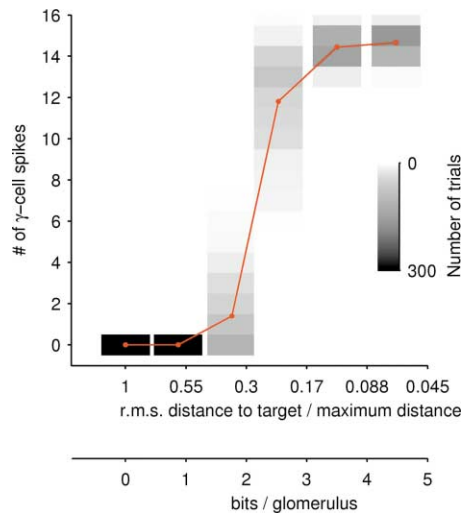


Figure 8. The Response of a  $\gamma$  Cell to Odors of Varying Degree of Similarity to the Target Odor, but Activating the Same Glomerular Set

Ensembles were generated with varying root-mean-square distances (for each component) from the target analog value. Statistics collected on 300 odors, with  $n = 0.87, 1.76, 2.53, 3.50,$  and  $4.48$  bits of information about the size of each analog component.  $N_{\text{glomeruli}} = 400$ . Distance in glomerular activation levels was normalized to the maximum possible distance.

Figure 8 plots the result of this study. The number of bits with which test odors must be specified in order to produce the same number of  $\gamma$  cell spikes as the ideal target is  $\sim 3.5$  bits. Thus, above 3.5 bits, test and target odors cannot be discriminated based on the number of  $\gamma$  cell spikes. In other words, the useful analog information per glomerulus saturates at  $\sim 3.5$  bits, which corresponds to dividing the full possible coverage range into about ten different levels.

For a system with  $N$  glomeruli, one could then in principle define  $10^N$  different odors. However, our recognition system intrinsically treats many of these  $10^N$  possibilities as being the same odor: for a  $\gamma$  cell to respond, only roughly half of its mitral cell inputs need to be well synchronized, meaning that half of the  $N$  glomerular inputs can be corrupted and the odor is still recognized. This is what allows the system to perform tasks such as recognizing a known odor in the presence of a strong unknown background. It is in this sense that we have not determined how many different odors the system can distinguish, but have merely found what precision is significant at the input to the system.

All of the test odors used in Figure 8 activate exactly the same glomeruli as the target odor. The leftmost column of Figure 8 shows that when the magnitudes of the components of the test odors are chosen entirely randomly (0 bits analog information), fewer than 1 odor in 300 will produce any spikes in a  $\gamma$  cell. To obtain a more stringent lower bound on the number of odors the system can distinguish through making use of analog values, we reran the test of the leftmost column of Figure 8, but now applied 3,000,000 different random test odors in a smaller system (for computational efficiency), with 280 glomeruli. No action potentials were generated by

any of the  $3 \times 10^6$  random odors. Selectivity grows with number of glomeruli; with 400 or more glomeruli, the functional selectivity due to analog information will be enormous. In the more natural case of random odors across all glomeruli (i.e., not always using the same set of glomeruli activated above threshold), the functional selectivity is even greater.

## Discussion

We have shown that noisy spiking neurons, using the many-are-equal (MAE) operation (Hopfield and Brody, 2000, 2001), can be configured, in a manner reminiscent of the anatomical and functional organization of the olfactory bulb, to solve some of the major computational problems faced by olfactory systems in a natural environment: recognition of odors over a range of concentrations and in the presence of distracting background odors. The many mitral cells that are part of each glomerulus are tuned to the same odors, but they provide a repertoire of different response strengths that are used here as the basis for representing, and computing with, analog signal strength. The presence of target odors is indicated by synchronization across a number of “mitral” cells in different glomeruli and is highly odor selective. This selective synchronization is invariant to a 50-fold change in concentration. Odor-selective synchronization still occurs in the presence of strong background odors, thus allowing odor segmentation and the decomposition of mixtures of known odors into their components.

The MAE operation allows a system to ignore badly contaminated information, as long as it does not affect too large a fraction of information channels. The use of MANY, rather than ALL, is essential to carrying out olfactory tasks, for a particular odorant can easily dominate many glomeruli while other glomeruli are responding to other odorants that are simultaneously present.

In this scheme, both the computational operation used (MAE) and the way sensory information is represented are essential. The relative activations between glomeruli are key to the definition of a target odor (Figure 5A) and allowed us here to obtain concentration-invariant recognition in the presence of background odors. (Both of these real-world requirements grossly perturb the pattern of glomeruli activated by a pure odor at a single, standard, concentration.) Differentiating between two individually presented random odors that have as much as 100% overlap in the identity of activated receptors is readily done (compare Figures 6A–6C to Figures 7A and 7B). In the situation more nearly resembling the natural olfactory background or mixture problems, the odors will have much less glomerular overlap, further simplifying the problem. More surprisingly, and thanks to the robustness to corrupted components of the MAE operation, the system can even separately recognize two *simultaneously* presented random odors with 100% glomerular overlap. Such problems would be totally intractable if odors were described merely by a “spatial pattern,” i.e., by the identity of the glomeruli excited above some fixed threshold. The system makes use of about 10 analog levels, or 3.5 bits of

information, for each glomerulus driven above threshold, in addition to the 1 bit per glomerulus available from “pattern” alone.

### Experimental Procedures

#### Receptor Responses and Concentration-Invariant Odor Encoding

The approach used here to obtain concentration-invariant recognition is based on logarithmic encoding of recognition by the glomeruli. However, it is generalizable to other situations. Let the activation of each receptor type  $r_i$  be given by some arbitrary but invertible function  $f_i$  that depends on both odor identity and odor concentration.

$$r_i = f_i(c_o; o)$$

The logarithmic encoding described above is a special case of this, where odor identity determines threshold and  $k_{oi}$ , and odor concentration determines activation. To test the hypothesis that some specific odor  $o$  is present, the functions  $f_i$  can be inverted to get an estimate, from each  $r_i$ , of the concentration of odor  $o$ .

$$c_{oi} = f_i^{-1}(r_i; o)$$

When odor  $o$  is present, the estimates  $c_{oi}$  will be the same across all receptors  $i$ . In contrast, when receptors are driven by a different odor,  $u$ , the estimates  $c_{oi}$  will be different to each other. This is true independent of concentration. Thus, an MAE operation on the estimates  $c_{oi}$  will result in concentration-invariant odor recognition.

The special case of logarithmic odor encoding permits concentration invariance without inverting the function  $f_i$ . There is a range over which this may correspond to the biological situation (Duchamp-Viret et al. 2000; Meister and Bonhoeffer 2001; Wachowiak and Cohen, 2001). However, for some other odor encodings, neural implementation of the inversion of  $f_i$  is also feasible. For example, if receptor activation depended linearly on odor concentration,  $r_i = k_{i,odor} c_{odor}$ , a variety of multiplicative synaptic weights from a receptor to the glomerular repertoire would replace the additive bias currents used in the logarithmic encoding case. To recognizing odor  $o$ , the mitral cell selected in glomerulus  $i$  would be the one that had synaptic weight most closely proportional to  $1/k_{io}$ . If odor encoding were quadratic, appropriate synaptic depression from receptors to repertoire cells could be used to invert  $f_i$ ; if odor encoding were proportional to the square root of concentration, synaptic facilitation could be used to invert  $f_i$ . In the absence of detailed knowledge, we use here the simplest assumption, logarithmic encoding, but the essence of the computation can readily be implemented biologically for other encodings as well.

#### Simulation Methods

Each odor  $o$  was defined by a set of binding constants  $k_{oi}$  to receptor types  $i$ . The logarithms (base 10) of the  $k_{oi}$  were each chosen randomly and uniformly over the range  $-7$  to  $-1$ , yielding a range of binding constants spanning a range of  $10^{-7}$  to  $10^{-1}$ . With this scale of binding constants, threshold coverage for activation of a glomerulus ( $\theta$  in equation 2) was defined as  $10^{-4}$ , so that an odor concentration  $c_o$  of 1.0 corresponded to the strength of odor at which half of the receptor types had coverages  $r_i = c_o k_{oi}$  that drove their corresponding glomeruli above threshold (Equation 2).

Each glomerulus received input from one receptor cell type and had its own ensemble of repertoire cells, each with its own constant bias current. The bias current for each repertoire cell was chosen from a uniform random distribution over the range of bias currents shown in Figure 1. For most of the simulations, 14 repertoire cells were assigned to each glomerulus.

Glomerular repertoire cells were modeled as leaky integrate-and-fire units with “action potentials” of negligible duration and time constants of 20 ms. Resting potential was 10 mV, and the threshold for action potential firing was 20 mV. After firing an action potential, membrane potential was held fixed at 0 mV for 2 ms (to simulate an absolute refractory period).  $\gamma$  cells were modeled with the same parameters, except their membrane time constant was 6 ms. Connections from repertoire cells to  $\gamma$  cells were modeled as producing

both an excitatory postsynaptic current (exponential,  $\tau = 2$  ms) and an inhibitory postsynaptic current ( $\alpha$  function,  $\tau = 6$  ms). The mediating inhibitory pathway that would in biology be responsible for such an inhibitory interaction was omitted for simplicity. Model cells with these same parameters were used in an earlier study (Hopfield and Brody, 2000, 2001). The strength of the inhibitory synapses was chosen so that the total charge that flowed into a  $\gamma$  cell due to an action potential in one of its repertoire cells was zero.

The sniff of duration 0.5 s was modeled as a half-sine wave. Thus, when a single odorant A was present, the coverage of receptors of type  $i$  was given by

$$r_i = (\sin[2\pi \times (t - t_{start})])(c_o k_{Ai}) \text{ if } t_{start} < t < t_{start} + 0.5, 0 \text{ otherwise.}$$

←-----→  
0.5-s-long sniff

When two odorants A and B were simultaneously presented, the net coverage was the sum

$$r_i = (\sin[2\pi \times (t - t_{start})])(c_o k_{Ai} + c_o k_{Bi}) \text{ if } t_{start} < t < t_{start} + 0.5, 0 \text{ otherwise.}$$

←-----→  
0.5-s-long sniff

One repertoire cell was chosen from each of these glomeruli to make a connection to the  $\gamma$  cell; the repertoire cell was chosen so that the sum of the bias current and the sensory input from odor A at concentration 1.0 was at the center of the range of input currents where the repertoire cells showed good phase-locking.

#### Acknowledgments

We thank Z.F. Mainen for discussion. This work was supported in part by grant number R01 DC06104-01 from the NIH.

Received: July 27, 2002

Revised: January 21, 2003

#### References

- Buck, L.B. (1996). Information coding in the vertebrate olfactory system. *Annu. Rev. Neurosci.* 19, 517–544.
- Buck, L., and Axel, R. (1991). A novel multigene family may encode odorant receptors—a molecular basis for odor recognition. *Cell* 65, 175–187.
- Desmaisons, D., Vincent, J., and Lledo, P.M. (1999). Control of action potential timing by intrinsic subthreshold oscillations in olfactory bulb output neurons. *J. Neurosci.* 19, 10727–10737.
- Duchamp-Viret, P., Duchamp, A., and Chaput, M.A. (2000). Peripheral odor coding in the rat and frog: quality and intensity specification. *J. Neurosci.* 20, 2383–2390.
- Hopfield, J.J. (1995). Pattern recognition computation using action potential timing for stimulus representation. *Nature* 376, 33–36.
- Hopfield, J.J. (1999). Odor space and olfactory processing: collective algorithms and neural implementation. *Proc. Natl. Acad. Sci. USA* 96, 12506–12511.
- Hopfield, J.J., and Brody, C.D. (2000). What is a moment? “Cortical” sensory integration over a brief interval. *Proc. Natl. Acad. Sci. USA* 97, 13919–13924.
- Hopfield, J.J., and Brody, C.D. (2001). What is a moment? Transient synchrony as a collective mechanism for spatiotemporal integration. *Proc. Natl. Acad. Sci. USA* 98, 1282–1287.
- Hopfield, J.J., Brody, C.D., and Roweis, S. (1998). Computing with action potentials. *Adv. Neural Inf. Process.* 10, 166–172.
- Johnson, D.H. (1980). The relationship between spike rate and synchrony in responses of auditory-nerve fibers to single tones. *J. Acoust. Soc. Am.* 68, 1115–1122.
- Kashiwadani, H., Sasaki, Y.F., Uchida, N., and Mori, K. (1999). Synchronized oscillatory discharges of mitral/tufted cells with different molecular receptive ranges in the rabbit olfactory bulb. *J. Neurophysiol.* 82, 1786–1792.
- Krone, D., Mannel, M., Pauli, E., and Hummel, T. (2001). Qualitative and quantitative olfactometric evaluation of different concentrations of ethanol peppermint oil solutions. *Phytother. Res.* 15, 135–138.

- Laing, D.G., and Francis, G.W. (1989). The capacity of humans to identify odors in mixtures. *Physiol. Behav.* *46*, 809–814.
- Laing, D.G., and Jinks, A.L. (2001). Psychophysical analysis of complex odor mixtures. *Chimia* *55*, 413–420.
- Lavine, R.A. (1971). Phase locking in response of single neurons in cochlear nucleus complex of the cat to low frequency tonal stimuli. *J. Neurophysiol.* *34*, 467–483.
- Meister, M., and Bonhoeffer, T. (2001). Tuning and topography in an odor map on the rat olfactory bulb. *J. Neurosci.* *21*, 1351–1360.
- Perez-Orive, J., Mazor, O., Turner, G.C., Cassenaer, S., Wilson, R.I., and Laurent, G. (2002). Oscillations and sparsening of odor representations in the mushroom body. *Science* *297*, 359–365.
- Rubin, B.D., and Katz, L.C. (1999). Optical imaging of odorant representations in the mammalian olfactory bulb. *Neuron* *23*, 499–511.
- Shepherd, G.M., and Greer, C.A. (1998). Olfactory Bulb. In *The Synaptic Organization of the Brain*, G.M. Shepherd, ed. (New York: Oxford University Press), pp. 159–204.
- Sicard, G., and Holley, A. (1984). Receptor cell responses to odorants—similarities and differences among odorants. *Brain Res.* *292*, 283–296.
- Wachowiak, M., and Cohen, L.B. (2001). Representation of odorants by receptor neuron input to the mouse olfactory bulb. *Neuron* *32*, 723–735.